Defence Technology xxx (2018) 1–13

Contents lists available at ScienceDirect

Defence Technology

journal homepage: www.elsevier.com/locate/dt

An overview on properties, thermal decomposition, and combustion behavior of ADN and ADN based solid propellants

Pratim Kumar

Alliance College of Engineering and Design, Alliance University, Bengaluru, India

A R T I C L E I N F O

Article history:
Received 19 January 2018
Received in revised form
10 March 2018
Accepted 29 March 2018
Available online xxx

Keywords:
ADN
Green oxidizer
Green propellant
Thermal decomposition
Combustion

A B S T R A C T

Ammonium dinitramide [$NH_4N(NO_2)_2$, ADN] is considered as a possible replacement for ammonium perchlorate (AP) in nearly all kind of solid rocket propulsions in the coming future. The reason to use ADN instead of AP in solid rocket propulsion is because of its harmless combustion products, along with its capacity to generate high specific impulse (Isp). ADN is fairly a new member in the solid oxidizer community and is considered under green energetic material (GEM). Application and feasible utilization of ADN as an oxidizer for composite solid propellants (CSP's) requires complete knowledge of its thermal decomposition processes along with its combustion behavior. A detailed overview on the physical and chemical properties, thermal decomposition, and combustion behavior of ADN and ADN based propellants has been discussed in this paper. Catalytic effect on thermal decomposition, combustion wave structure, and burning rate of ADN is also discussed.

1. Introduction

ADN was first synthesized in 1971 at the Zelinsky Institute of Organic Chemistry in Moscow, USSR, and is one of the most noteworthy discoveries in the field of energetic materials [1]. It was claimed that, ADN-based solid propellants are in use under Russian Topol intercontinental ballistic missiles in the former USSR. The USSR's dinitramide technology was strictly confidential and was unknown to the rest of the world till 1988. ADN was “re-invented” at SRI (*Stanford Research Institute*), USA in the year 1988 again. And, in the beginning of the 1990's, FOI (Forskningsinstitut/Swedish Defense Research Agency) in Sweden started research on ADN in order to develop high performance solid propellants.

At present, ammonium perchlorate (AP) and hydrazine are the widely used propellant ingredient in modern rocketry. AP is one of the major constituent as an oxidizer in solid propellants, while hydrazine in liquid monopropellant or bi-propellant liquid rockets. These propellants are well known for their high performance, good combustion characteristics, high thrust, easily availability, and low cost. With these advantages, both possess some disadvantages too. All of these chemicals are extremely toxic and have carcinogenic effects on the human health. Both are also unsafe for the environment, requires safe operational handling, and also need safe storage conditions.

Ammonium dinitramide (ADN) [$NH_4N(NO_2)_2$] is one of the newest member in solid propellant community as an oxidizer entity which has the potential to replace ammonium perchlorate (AP) fully or partially in nearly all kind of solid rocket propulsion. ADN is one of the capable oxidizer with high specific impulse (Isp) and high burning rate ($\dot{r}$) [2]. At present, AP is a workhorse oxidizer for solid rocket propulsion. The reason for frequent use of AP are its, a) high burning rate, b) non-hygroscopic crystals, c) burning rate tailoring capacity, and d) easy compatibility with various fuel binders. Although, combustion of AP produces carcinogenic compounds along with chlorine (Cl_2) gas and various chlorine oxides (ClOx) [3]. All these combustion products of AP are detrimental for the earth environment and for its flora and fauna.

In the recent years, frequency of rocket launch has increases considerably due to the advancement in the space technology, space exploration, space tourism, and for conducting space based zero-gravity experiments at International Space Station (ISS). Most of the rocket use solid propellant in their booster stage, as solid propellant has the capability to produce sufficient thrust in a very short period of time. In booster stage, AP based CSP's are used for generating high thrust. As an example, European Space Launcher Ariane-5 contains 476 tons of AP based CSP, which converts into 270 tons of concentrated HCl upon combustion [1]. Hence, regular use of AP can lead to detrimental effects on earth atmosphere and

E-mail addresses: pratim.kumar.86@gmail.com, pratim.kumar@alliance.edu.in.
Peer review under responsibility of China Ordnance Society

https://doi.org/10.1016/j.dt.2018.03.009

on the upper ozone layer. Because of such reasons, development of ADN based CSP's is necessary to replace AP based CSP's in the coming future.

ADN mainly consist nitrogen (N), oxygen (O), and hydrogen (H) in its molecular structure. Hence, combustion products of ADN are harmless to the environment. Further, presence of dinitramide anion [$N(NO_2)_2^-$] imparts high density, high heat of formation, high oxygen balance, and high oxygen content [4]. However, ADN also suffers from many drawbacks too like, a) fairly high sensitivity crystals, b) costly synthesis, and c) sensitivity towards light and moisture. ADN derive most of its energy from their very high positive heat of formation rather than from the oxidation of the carbon backbone as in the case of conventional energetic materials [5]. The low percentage of carbon and hydrogen in these compounds induces following effects, a) Increase the density, b) good oxygen balance, and c) produce more moles of gaseous products per gram upon combustion.

Hence, for the viable use of ADN in propellant formulations and in other applications, detailed information over its thermal properties and decomposition behavior is compulsory. Present work is a compilation of all the physical and chemical properties, decomposition process, and burning behavior of ADN and ADN based propellants from some of the important and noteworthy technical research papers over ADN.

2. Properties

ADN is a solid white salt of the ammonia cation (NH_4^+) and the dinitramide anion [$N(NO_2)_2^-$]. It has a high oxygen balance (OB) of 25.8%, melting point at 93 °C, and decomposition temperature of 150 °C. ADN is a hygroscopic and readily soluble crystal in water and in other polar solvents, but scarcely soluble in non-polar solvents. The critical relative humidity (CRH) for ADN is 55.2% at 25.0 °C. The density of ADN in the solid state is 1.81 g/cm^3. Its molar volume and corresponding density in liquid state at 25.0 °C is 74.08 g/mol and 1.675 g/cm respectively [1].

Melting point of ADN is 91–93 °C [6–10], and its decomposition completes by 200 °C. ADN shows endothermic melting peak at 91–93 °C, followed by an exothermic decomposition in a range of 150–210 °C, and again one endothermic decomposition of ammonium nitrate (AN) *in-situ* formed during the decomposition of ADN. TGA of ADN showed single stage decomposition with 100% mass loss by 220 °C.

The oxygen balance of ADN is 25.8%, lower than the 34% of AP. This disadvantage is compensated by its high heat of formation (−125.3 kJ/mol) when compared to (−283.1 kJ/mol) of AP. The density of the ADN crystals is 1.885 g/cm^3, lower than 1.950 g/cm^3 of AP. However, ADN hygroscopicity and impact sensitivity are higher than that of AP [11].

ADN is a water soluble ionic salt, hence UV-Visible spectrometry is one of the best method for analyzing ADN crystals. The UV spectrum of ADN was characterized by two peaks at 214 and 284 nm. Absorbance at 284 nm is the characteristics of $-N(NO_2)^-$ ion due to the low energy n-π^* transition, and the absorption maximum at 214 nm is due to high energy σ-σ^* transition [12].

3. Decomposition

The initial decomposition step of ammonium salts is their dissociation into ammonia and the corresponding acid [13,14]. Some of the examples are, ammonium nitrate (AN), ammonium perchlorate (AP), and ammonium dinitramide (ADN). AN decomposes into NH_3 and HNO_3 (nitric acid), AP decomposes into NH_3 and $HClO_4$ (perchloric acid), and ADN decomposes into NH_3 and $HN(NO_2)_2$ (dinitramidic acid). The next decomposition step is temperature controlled i.e. at different temperature the decomposition pathways changes. The initial step in the thermal decomposition of ADN has been suggested as follows [15]:

a) Conversion to ammonium nitrate (AN) and nitrogen di-oxide (NO_2).
b) Sublimation into NH_3 and $HN(NO_2)_2$.
c) Dissociation of the dinitramide ion, $N(NO_2)_2^-$, through the loss of either NO_2 or NO_2^-.
d) Conversion of the dinitramide ion to N_2O and NO_3^-.

These initial steps are followed by series of subsequent reactions leading to products that may include combinations of HNO_3, N_2O, NO_2, NH_3, H_2O, NO, HNO_2, N_2 etc.

In general, differential scanning calorimetry (DSC) plot of ADN consisted of two exothermic and two endothermic peaks [6–10,16,17]. First endothermic peak (91–94 °C) was for the melting of ADN, first exothermic peak (160–190 °C) was for the dissociation of ADN into ammonium nitrate (AN) and nitrous oxide (N_2O), second exothermic peak was for AN dissociation (274 °C), and one more endothermic peak at (300 °C) was due to the formation and vaporization of water during AN decomposition [13]. Similarly, another important dinitramide based oxidizer i.e. potassium dinitramide (KDN) DSC plot also shows two endothermic peaks and one exothermic peak [18]. Two endothermic peaks are for KDN, and potassium nitrate (KNO_3) decomposition, while one exothermic decomposition peak was for the KDN decomposition into KNO_3 and N_2O.

Yang et al. [19], presented a comprehensive review on thermal decomposition and combustion of ammonium dinitramide (ADN). Thermal decomposition processes of ADN depend strongly on the pressure, temperature, and experimental methods. Decomposition of ADN is an acid-catalytic and self accelerated, but retarded by water and base [9,20]. Rossi et al. [21], conducted thermal decomposition studies of ADN in a vacuum chamber and monitored the evolved gas by a quadrupole mass spectrometer (TG-QMS). Authors of Ref. [21] suggested three reaction paths for thermal decomposition of ADN:

$$NH_4N(NO_2)_2 \rightarrow NH_3 + HN(NO_2)_2 \rightarrow NH_3 + HNO_3 + N_2O$$

$$NH_4N(NO_2)_2 \rightarrow (2NH_2NO_2) \rightarrow 2N_2O + 2H_2O$$

$$NH_4N(NO_2)_2 \rightarrow NH_4NO_3 + N_2O$$

Ermolin [22], worked out on modeling of pyrolysis of ADN sublimation products under low pressure (10 torr) and in a temperature range of 373–920 K. The computations were carried out under the assumption that ADN sublimation proceeds as, ADN → NH_3 + $HN(NO_2)_2$. By comparing the numerical and experimental data, contributions of individual stages and components to the chemical process, authors evaluated the rate constants of three reactions. The reactions with their rate constants are:

$$HNNO_2 + NO \rightarrow NO_2 + HNNO \ (10^8)$$

$$HNNO_2 + NO_2 \rightarrow HNO + NO + NO_2 \ (3 \times 10^9)$$

$$HNNO + NO \rightarrow N_2H + HNO_2 \ (3.2 \times 10^{-6})$$

Park et al. [23], studied thermal decomposition of ADN in the gas phase at 373–970 K by pyrolysis/MS under low conditions using a Saalfield reactor. According to them, following elementary reactions play a key role in a low-pressure condition:

Chain initiation reactions:

Please cite this article in press as: Kumar P, , An overview on properties, thermal decomposition, and combustion behavior of ADN and ADN based solid propellants, Defence Technology (2018), https://doi.org/10.1016/j.dt.2018.03.009

$HN(NO_2)_2 \rightarrow HNNO_2 + NO_2$

$HNNO_2 + M \rightarrow OH + N_2O + M$

Chain propagation reactions:

$OH + NH_3 \rightarrow H_2O + NH_2$

$NH_2 + NO_2 \rightarrow H_2NO + NO$

$NH_2 + NO \rightarrow H + N_2 + OH$

Under high pressure conditions, they suggested the following radical-radical reactions involving $HNNO_2$ to become significant because of the increasing concentrations of radical species:

$$\begin{aligned} HNNO_2 + OH &\rightarrow HNOH + NO_2 \\ &\rightarrow HNO + HONO \\ HNNO_2 + NO &\rightarrow HNNO + NO_2 \\ &\rightarrow HONO + N_2O \\ HNNO_2 + NO_2 &\rightarrow HNO + N_2O_3 (NO + NO_2) \\ &\rightarrow HNO_3 + N_2O \end{aligned}$$

Rahm et al. [24,25], used quantum chemical modeling of molecular clusters to investigate the thermal decomposition of ADN and KDN under atmospheric and sub-atmospheric conditions. The rate determining steps for ADN and KDN are their dissociation into NO_2 and NNO_2^- radicals. The activation barriers for these steps are 30 and 36 kcal/mol for ADN and KDN respectively. Decomposition barrier for HDN in the gas-phase is 38 kcal/mol. The decomposition is governed by surface chemical processes, involving polarized dinitramide anions of reduced stability. There model successfully explained the decomposition of ADN into NO_2, NO_3, NO, N_2O, H_2O, NH_3, and NH_4NO_3 as suggested in Ref. [26].

Shmakov et al. [27], studied thermal decomposition of ADN using two-temperature flow reactor at 800 Pa. The calculated heat of vaporization of ADN was 155.4 ± 12.6 kJ/mol, and vapor pressure of ADN at 80, 115, 130 and 140 °C are $(0.67–1.3)\cdot 10^{-2}$, 0.21, 2.8 and 9.3 respectively. From the obtained values, they proposed a mechanism for the thermal decomposition of ADN, which includes the ADN vaporization stage i.e. the transition from the condensed to the gaseous state in the form of molecular complex $NH_3 \cdot HN(NO_2)_2$ (ADN vapor) followed by dissociation into NH_3 and HDN. The values of degree of ADN decomposition (α) and effective decomposition rate constant (k_{eff}, s^{-1}) at 800 Pa for 140, 160, 200, 240 and 320 °C are (0,-), (0.1, 3.1), (0.21, 7.8), (0.32, 14.0) and (0.82, 71.8) respectively.

Brill et al. [28], studied ADN decomposition at 2000 °C/s, and detected decomposition products with the help of T-jump/FTIR technique. ADN undergoes rapid decomposition process which was highly exothermic due to the formation of large amount of NH_3 and N_2O in the early decomposition stage. In the experiment, ADN was heated up to 260 °C with the heating rate of 2000 °C/s. During the initial stage of ADN decomposition equal amount of HNO_3, NH_3, and N_2O formed. In the middle, mole concentrations of N_2O, NO_2, and AN increase while that of NH_3 and HNO_3 decreases. At the end of the decomposition, the mole concentrations of N_2O and NH_3 increases, HNO_3 decreases and NO_2, NO and AN remains constant.

Vyazovkin et al. [29], studies decomposition of ADN under heating rate of 0.02 °C/s and 10^7 °C/s. Heating rate of 10^7 °C/s was achieved by pulsed CO_2 laser heating and the final temperature was 630 °C. The thermal decomposition products were monitored by FTIR spectroscopy. At the heating rate of 1.5–20 °C/min the maximum temperature reached up to 250 °C. The observed gaseous decomposition products in this case are N_2O, NO_2, NO, NH_3 and HNO_3. The gases were monitored by their respective absorption bands at 2224, 1621, 1903, 966 and 1709 cm^{-1} respectively. Under high heating rate, the primary condensed phase decomposition products are N_2O and NO_2, which are followed by NO at a later stage. They finally concluded that, ADN decomposition mechanism can be used to model the decomposition of ADN under the extreme conditions too like that of combustion of solid rocket propellants.

Vyazovkin et al. [16], studied ADN decomposition by DSC and TGA coupled with TG-MS. Overall heat release in the decomposition temperature range of 130–230 °C for ADN was 240 ± 20 kJ/mol. The identified evolved gases are NH_3, H_2O, NO, N_2O, NO_2 and HNO_3 as suggested in Refs. [24,26,28,29], and one more identified gas was HONO. Initially the global activation energy for ADN was 175 ± 20 kJ/mol, which decreases to 125 ± 20 kJ/mol at the completion of the reaction. They detected the presence of NO, N_2O and NO_2 in the early stage of decomposition, but as compare to other experiments [21,28] authors detected the presence of NH_3 relatively late in the decomposition process. One of the reasons is that they carried out the experiments in open aluminum pan which favors condensed phase mechanism.

Zhu et al. [30], investigated mechanism for sublimation of ADN quantum-mechanically. There results show that three steps involved in the sublimation/decomposition of ADN. The steps are:

a) Relaxation of the surface layer with 1.6 kcal/mol energy per $NH_4ON(O)NNO_2$ unit.
b) Sublimation of the surface layer to form a molecular $[NH_3]$-$[HON(O)NNO_2]$ complex with a 29.4 kcal/mol sublimation energy.
c) Dissociation of the $[H_3N]$-$[HON(O)NNO_2]$ complex to give NH_3 and $HON(O)NNO_2$ with the dissociation energy of 13.9 kcal/mol.

The total calculated sublimation enthalpy for ADN(s) → NH_3(g) + $HON(O)NNO_2$ (g) was 44.9 kcal/mol via 3 steps. They also studied the effect of H_2O on the sublimation process on ADN and AP. The sublimation enthalpies for $(H_2O)x–NH_4/N_3O_4$ (x = 0,1,2,3) were 29.4, 32.6, 32.8 and 30 kcal/mol, while for AP it was 28.1, 21.4, 18.6 and 14.2 kcal/mol.

Lobbecke et al. [31], investigated on the DSC and TGA plot of ADN. TGA plot shows a mass decrease of 30% in first step (ADN → AN + N_2O) and 70% mass loss in 2nd step for ADN (conversion of ADN into gaseous products). At higher temperatures, ADN decomposes into N_2O and H_2O. The decrease of AN at T > 200 °C and the increase of N_2O in a second evaporation step were detected by evolved gas analysis.

$$\begin{aligned} NH_4N(NO_2)_2 &\rightarrow NH_3 + HN(NO_2)_2 \\ &\rightarrow NH_3 + HNO_3 + N_2O \\ &\rightarrow NH_4NO_3 + N_2O \\ NH_4NO_3 &\rightarrow N_2O + 2H_2O. \end{aligned}$$

Along with the main decomposition pathways as shown above, they also suggested different side reactions taking place to form NO_2, N_2O, NO, N_2 and O_2. The important side reactions are summarized as follows:

Please cite this article in press as: Kumar P, , An overview on properties, thermal decomposition, and combustion behavior of ADN and ADN based solid propellants, Defence Technology (2018), https://doi.org/10.1016/j.dt.2018.03.009

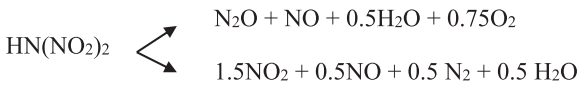

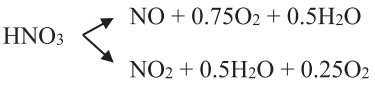

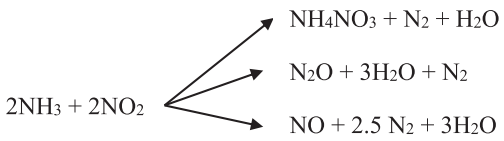

$2\ NH_3 + 3N_2O \rightarrow 3\ H_2O + 4N_2$

$2NO_2 + H_2O \rightarrow HNO_3 + HNO_2$

$2\ NH_3 + 3N_2O \rightarrow 3H_2O + 4N_2$

$2NO_2 + H_2O \rightarrow HNO_3 + HNO_2$

Oxley et al. [13], studied thermal decomposition of pure ADN and in solution. The decomposition of pure ADN releases N_2 and N_2O in equal ratios of 0.85 mol each gas/l mol of ADN at 230 °C. The ratio shifts during the course of the reaction and with temperature, but for N_2/N_2O it lies in the ratio of 0.6–0.8, with the total amount of gas being about 1.6–1.7 mol per mole ADN. In aqueous solutions ADN forms primarily N_2O (200 °C, N_2, 0.15 mol/mol; N_2O, 0.69 mol/mol). They give the following stoichiometry equation for ADN decomposition, $NH_4N(NO_2)_2 \rightarrow 0.44\ N_2 + 0.65\ N_2O + 0.68\ NH_4 + 0.22\ N(NO_2)_2^- + 0.46\ NO_3^-$. In their experiments they didn't detected the presence of NO_2 in thermolysis of ADN, while many researchers observed the presence of NO_2 [16,28,29]. The reason being suggested by them is that they carried out all experiments in a sealed glass capillary, in which ADN follows first order reaction with high degrees of conversion. They concluded that either the NO_2 does not catalyze ADN decomposition or it is not formed in large amounts. When HNO_3, AN, ADN or $(NH_4)_2SO_4$ was added to KDN, the exotherm was lowered to a temperature similar to the exotherm of ADN. These observations suggest that protons assist the decomposition of dinitramide.

Pavlov et al. [14,26], studied thermal decomposition of some other dinitramide onium salts [14] and of ammonium dinitramide [26] with its mechanism. In his first paper [14], the studied DNA salts are, a) hydrazinium b) binary ethylene-diammonium, c) trimethylammonium, d) guanidinium, e) anilinium, f) binary o-phenylenediammonium, g) tetramethylammonium, and h) tetra(n-butyl) ammonium salts. Their data's showed that the mechanism of decomposition of DNA onium salts depends on pKa of the salt-forming base. When pKa >7, the decomposition occurs, via the cleavage of the N-N bond with elimination of NO_2, and when pKa <5, the primary dissociation of the salt to the base and acid predominates. In Ref. [26], the kinetics of thermal decomposition of ADN was studied by manometric method. The reactions were carried out in 0.2–10 cm^3 glass vessels with crescent like membranes. They investigated the decomposition of ADN melt and ADN in the solid phase. Composition of the gaseous products of ADN melt at various temperatures was measured by Gas Chromatographic (GC) technique. At all the temperature (104–170 °C), percentage of N_2 and N_2O were maximum, and presence of H_2O and NO_2 was in traces. AN and water was always present as an admixture in ADN. Melting point for AN:ADN = 1:2 is 60 °C. Low amounts of water (<0.5%) doesn't accelerate the decomposition.

Matsunaga et al. [32,33] has studied the thermal decomposition behavior of ADN in high pressure [32] and in the presence of cupric oxide [33] separately. In Ref. [32], the selected pressure range for studying the ADN decomposition was 0.1 MPa–6 MPa. DSC, TG, and gas analysis were performed using PSDC and Raman spectrometry techniques. It was found that, exothermic decomposition of ADN increases with increase in pressure. Also, AN inhibits the decomposition of ADN at low temperatures, and promotes exothermicity at high temperatures. At low pressure, AN was produced at the same time as the start of exothermic decomposition. At initial stage, thermal decomposition of ADN that does not generate AN, although AN generation was increased by increase in pressure. In Ref. [33], ADN + CuO sample was used for studying the thermal decomposition process. From experiment, it was observed that copper dinitramide, $Cu[N(NO_2)_2]_2$ was generated at the surface of CuO. Cupric oxide and copper dinitramide further breaks into $[Cu(NH_3)_2](NO_3)_2]$ and $Cu(NO_3)_2$, which is exothermic in nature.

Some other latest articles over kinetics [34,35], and ionization [36] of ADN provided the detailed activation energy values of various decomposition steps of ADN, and adiabatic ionization potentials of ADN decomposition. Ermolin [37], also presented a detailed review over the thermal decomposition of ADN. It was found that dinitramide anion, $N(NO2)^-$ play a major role in ADN decomposition.

In a gist, it can be said that the thermal decomposition of ADN and other dinitramide salts exhibit characteristics of base stability and acid catalysis. HNO_3 is one of the decomposition products of ADN, and the addition of HNO_3 aqueous solution to the ADN melt accelerates decomposition. In strong acids, such as H_2SO_4, and HNO_3, ADN decomposes more rapidly at room temperature as the rate of acid-catalytic decomposition is proportional to acidity. The NO_2 gas was found to catalyze ADN decomposition, whereas the basic substances, such as NH_3, NH_4F, amine, and urea may restrain ADN decomposition. NH_3, $HN(NO_2)_2$, $HNNO_2$, HNO_3, N_2O, NO_2, NO, H_2O, N_2 and AN are found to be the prominent decomposition products of ADN pyrolysis, and their evolution rates depend on temperature and pressure. N_2O evolution is one of the main characteristics of ADN thermal decomposition. At low temperatures or in vacuum, ADN decomposition produces only small amounts of N_2 and H_2O. Under fast pyrolysis, N_2, and H_2O were formed in large amounts.

4. Combustion of ADN as oxidizer

Development of powerful ADN based green solid propellants is an interesting research in modern rocketry. As discussed in the introduction section, ADN possess high burning rate and non-chlorinated exhaust. In comparison with other energetic materials such as HNF, HMX, RDX, AP, AN, and CL-20, ADN shows promising good ballistic properties below 100 atmospheric pressure because of the large heat release in condensed phase [19]. Most of recent researches over ADN are focused on the combustion studies of ADN and ADN pellets, ADN/binder sandwiches, and ADN based CSP's.

Sinditskii et al. [38–40], in his set of three papers have presented the burning behavior and combustion mechanism of ADN. The combustion behavior of ADN was studied in the form of press strands (into quartz tubes, and into plexiglass tubes), ADN press pellets, and ADN single crystals. Burning rate analysis of condensed

Please cite this article in press as: Kumar P, , An overview on properties, thermal decomposition, and combustion behavior of ADN and ADN based solid propellants, Defence Technology (2018), https://doi.org/10.1016/j.dt.2018.03.009

products of ADN combustion, and effect of initial temperature on the burning rate were carried out for all the ADN samples in the pressure range of 0.1 MPa–40 MPa. ADN burns without any luminous emission at low pressure, forming copious white vapors, which condense as a fine white powder inside the tube and on the cold surfaces of the bomb. As the pressure increased, small "flamelets" emanated from the local reaction sites [41]. Above 1–2 MPa, the gases become almost transparent, a luminous flame appears, and the condensed products of combustion are not observed. At atmospheric pressure, authors failed to obtain self-sustained burning of pure ADN either by decreasing or increasing the sample diameter. Even at 80 °C, samples of pure ADN were incapable of complete burning at atmospheric pressures. Samples of molten ADN at a temperature of 100 °C was capable of complete burning with the burning rate varied from 6.7 to 9.1 mm/s.

Addition of 0.2% of paraffin to crystalline ADN changes the low pressure deflagration limit (LPDL) limit from 0.2 MPa to 0.02 MPa. Similarly, mixture of ADN with 0.2% of paraffin pressed into 7 mm plexiglass tubes was capable of sustained burning at atmospheric pressure even at initial temperature as low as 77 K (b.p. of nitrogen). The effect of small paraffin additive on the ADN burning rate characteristics could be explained by the fact that paraffin apparently shows itself as an alternative fuel, which is more readily oxidizable than NH_3. Apart from paraffin, halocarbon oil (which is not an oxidizable fuel) and SiO_2 (non–combustible) also reduces the LPDL limit, while soot (stabilizes combustion) can't able to reduce the LPDL limit. Hence, it was concluded that the LPDL limit is connected with physical reasons rather than the chemical ones for ADN.

Combustion of paraffin doped ADN at sub-atmospheric pressure is characterized by the lack of a luminous flame and the formation of copious condensed gas products. At atmospheric pressure paraffin doped ADN results in the formation of 47% weight percent of condensed-phase products. Authors found that condensed residue after ADN combustion at low pressures consists of a mixture of AN and ADN, with the ADN content increases as the pressure decreases. At atmospheric pressure, the ADN content of the residue after combustion of 0.2% paraffin doped ADN was 6% by weight.

Burning rate curves for all ADN pressed strands shows three segments with pressure. The first one from 0.2 MPa to 5.8 MPa in which burning rate increases, the second one from 5.8 MPa to 10 MPa in which burning rate decreases, and the last segment is of 10–36 MPa in which burning rate increases again. This erratic behavior of ADN combustion was explained by Sinditskii [42,43], and he proposed a qualitative theory for the three segments on ADN's burning rate vs. pressure curve. The theory is described in next paragraph.

At lower pressure (<20 atm), ADN combustion is marked by a large exothermic condensed-phase heat release (about 50 kcal/mol). Temperature gradient is also low on the surface of ADN at low pressures, and hence, there is negligible heat feedback from the gas phase in the first region of combustion. Therefore, Sinditskii proposed that condensed phase decomposition controls the first region of combustion; the gas phase flame having negligible or no impact. Because of high burning rate, condensed-phase material i.e. liquid droplets are dispersed into the gas phases and decompose there. Dispersion of condensed materials was observed for substances in which condensed phase decomposition dominates the combustion process [40,44]. With the increase in pressure, the dissociation temperature of ADN increases as well as energy required for dissociation. However, the condensed phase heat release does not increase with pressure in this region, and the gas phase still does not contribute significantly. This results in a growing deficiency of energy that was required to heat up and evaporate the condensed phase materials. To remove all of the condensed phase materials with pressure, the dispersion rate increases and this causes a decrease in the burning rate in second segment. Finally above 100 atm, stable combustion again achieved as the flame is now closer enough to the surface providing significant heat feedback and support combustion by augmenting the condensed phase heat release.

In his 2nd part [39], Sinditskii investigated on the possible combustion mechanism of ADN. At low pressure, the decomposition reaction of ADN to form condensed AN and gaseous N_2O at the surface via ionic reaction:

$$ADN\ (l) \rightarrow AN\ (l) + N_2O + 33\ kcal/mol$$

$$AN\ (l) \rightarrow HNO_3 + NH_3$$

Dissociation of AN into nitric acid and ammonia governs the surface temperature of ADN. ADN combustion at low pressure consists of AN and ADN mixtures, with the ADN content increases as the pressure decreases. Thermocouple measurements shows that the aerosol zone contains molten AN and ADN up to 2 MPa. With the rise in pressure, flame distances decreases, and decomposition completeness increases, resulting in the disappearance of condensed combustion products. In the gas phase and condensed phase, ADN decomposition forms extremely unstable dinitramidic acid, according to the reaction which are dissociative reactions:

$$ADN\ (l) \Leftrightarrow HDN\ (l) + NH_3\ (l)$$

$$HDN\ (g/l) \rightarrow NO_2 + HNNO_2 \rightarrow OH + N_2O$$

The radicals formed in the above reaction reacts with gaseous NH_3 dissolved in the melt and produces more than 50 kcal/mol, as a result of formation of gaseous water, nitrogen, nitrogen oxides, and nitric acid.

$$NO_2/\ OH + NH_3 \rightarrow H_2O, N_2, NO, N_2O$$

$$ADN\ (l) \rightarrow NH_4NNO_2\ (Ammonium\ nitrite) + NO_2 \rightarrow AN\ (l) + 2NO \rightarrow 2H_2O + 2NO + N_2 + 41\ kcal/mol.$$

The dissociation temperature of ammonium nitrite is lower than that of the other ammonium salts, ADN and AN. If ammonium nitrite substantially existed at the burning surface temperature would have been controlled by its dissociation reaction.

Once ADN droplets have dissociated, the temperature increases to form the first flame. This flame includes reaction of oxidation of ammonia by nitric acid decomposition products i.e. OH, NO_2. The temperature of the zone, however, does not correspond to the full heat release owing to N_2O and NO remaining partially unreacted in the flame. The combustion reaction reaches its total completion only in the 2nd flame, which was practically observed at 10 MPa, while it could be observed at lower pressures also at higher standoff distances. Schematic representation of the ADN flame structure is shown in Fig. 1.

The ADN combustion mechanism includes the fast decomposition reaction in the condensed phase to result in an aerosol flow above the surface and slow reactions in the gas. The ADN combustion can be satisfactorily described by a condensed phase combustion model with the rate controlling reaction being the ADN decomposition in the melt at low pressures (up to 1 MPa) and a gas phase model at high pressures (above 10 MPa), with the rate controlling reaction being HNO_3 in the first flame.

Combustion which was controlled by condensed phase reactions are basically divided into two groups [45]. First group considers the complete transformation of material in the

Please cite this article in press as: Kumar P, , An overview on properties, thermal decomposition, and combustion behavior of ADN and ADN based solid propellants, Defence Technology (2018), https://doi.org/10.1016/j.dt.2018.03.009

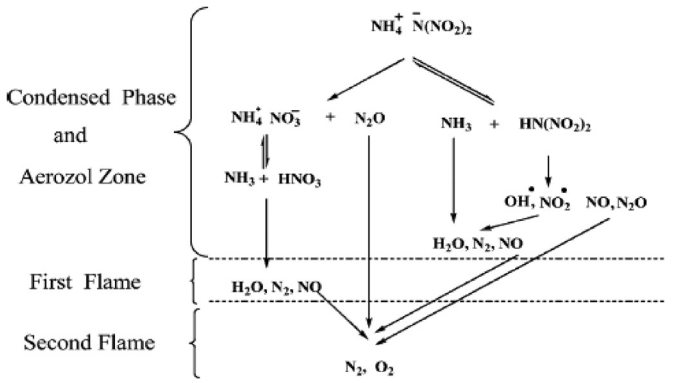

Fig. 1. Schematic representation of ADN flame structure [39].

combustion wave i.e. the wave propagation velocity is determined by the maximum combustion temperature, Tmax = To + Q/cp. In the second group, the burning surface is formed due to the physiochemical processes. The surface temperature (Ts) and the depth of the reactions (η) on the surface correspond to the incomplete conversion of the material and determine the burning rate. Combustion of various energetic materials capable of vaporization can be satisfactorily described using the c-phase model of the 2nd kind.

Flameless combustion is characteristics of energetic material at low pressures. As the pressure increases a high temperature flame appears. Combustion is controlled by c-phase reactions if the heat flux from the gas phase can be neglected i.e. if the heat flux from the gas phase is much smaller than the heat flux into the depth of the condensed phase. The most important parameters of the c-phase model are the surface temperature and the kinetics of the c-phase reaction controlling the burning rate.

Sinditskii [40], reported the rate constants of the rate-controlling reactions reaction of ADN combustion in the range of 0.02–1 MPa. The obtained value of rate constant (k) was,

$$k = 10^{16.37} \exp(-39{,}000/RT)$$

The obtained value is in good agreement with the decomposition kinetics of ADN found by other methods i.e. from the rate of disappearance of the dinitramide anion and the ammonium cation [13] [$k = 10^{16.94}$ exp (−39900/RT), and $k = 10^{15.56}$ exp (−37 800/RT)], and the rate of formation of gaseous products of decomposition [13] ($k = 10^{14.4}$ exp (−35 500/RT). All data in the range of T = 370–977 K are described by the single dependence, $k = 10^{16.16}$ exp (−38500/RT).

Fujisato et al. [46], studied the thermal decomposition behavior and combustion characteristics of mixtures of ADN with additives. The selected micro-meter sized particles of Al, Fe_2O_3, TiO_2, NiO, $Cu(OH)NO_3$, copper, CuO, and nano-meter sized particles of aluminum (Alex) and CuO (nano-CuO) were employed. The copper compounds and NiO lowered the onset temperature of ADN decomposition. The heat value of ADN with alex was larger than that of pure ADN in closed conditions. CuO and NiO enhance the burning rate particularly at pressures lower than 1 MPa because of the catalyzed decomposition in the condensed phase. Nano-CuO increase the burning surface temperature because of the contribution of the exothermic reactions exceeds the negative effects from the physical phenomena. While other additives lowers the burning rate. The decrease in burning rate was due to the chemical reaction taking place on the propellant surface, a phase change of the ammonium nitrate, and the blown −off droplets of the condensed phase. Alex and inert additives lowered the burning surface because of the endothermal physical effects were increased, which causes a negative effect on the burning rate. Author concluded that the balance of the reaction and the physical phenomena affect the burning surface temperature of ADN; therefore, inert additive particles decrease the burning rate by increasing the endothermic physical contributions. Reactive additives can enhance the burning rate by increasing the contribution from the exothermic reactions. These reactive particles also have the some endothermic physical effects, and the total effect is determined by the balance of these physicochemical phenomena.

Strunin et al. [47], determines the, a) burning rate as a function of pressure (0.066 MPa–6 MPa) and different additives (Cu_2O, $K_2Cr_2O_7$, Al, hydrocarbon fuels, rubber and plasticizer), b) temperatures in the combustion front, and c) the composition of the combustion products. The samples were prepared by pressing ADN under a pressure of 300 MPa into polymethylmethacrylate (PMMA). At pressure up to 1 MPa, combustion was without any luminous flame, but with the formation of great amount of white smoke [38,39]. The burning rate for the pressure range of 0.025–2 MPa are in agreement with de-Vielle's law ($r = ap^n$) with a pressure co-efficient (n) of about 0.7. The relative concentrations of NO, N_2O, NO_2, and HNO_3 remains constant at all the pressures, while that of N_2 increases above 0.05 MPa. The amount of AN, ammonium nitrite, and ADN decrease and that of H_2O increases with increase in pressure. Out of all additives, only Cu_2O (2%) leads to increase in the burning rate at low pressures, followed by decrease in it above 4 MPa. Reaction in ADN combustion at 0.066 MPa is presented by the equation:

$$\text{ADN} \rightarrow 0.412\ \text{AN} + .0004\ NH_4NO_2 + .007\ \text{ADN} + 0.338\ N_2O + 0.868\ \text{NO} + 0.331\ NO_2 + 1.178H_2O + 0.698\ N_2$$

Ermolin et al. [48], numerically simulated the chemical processes in the ADN flame between pressure ranges of 0.4–60 atm. From the obtained experimental data from his previous paper [22] and from other decomposition studies of ADN [15,17,21,23], the author estimated the role of HDN, aerosols, and ADN vapor in heat release in the ADN flame zone adjacent to the burning surface. The calculations predicted that the main source of heat release in the cold flame zone at p ≥ 3 atm is dinitramidic acid incoming through the channel of dissociative evaporation, ADN(l) → NH_3 + HDN from the burning surface. In the high temperature flame zone or in second flame zone, heat release was caused by the reaction that occurs in the $NH_3/N_2O/NO/NO_2/HNO_2/HNO_3$ mixture. At moderate pressures, the high temperature and low temperature zones are separated by an induction zone. OH radical, which plays an important role in the combustion, was produced in the induction zone by the following reaction, HNO_3 + M → OH + NO_2 + M. The produced OH radical consumed in the reaction, NH_3 + OH → NH_2 + H_2O. The high activation energy of this reaction led to small temperature disturbances in the induction zone at low pressures which cause finite change in the stand-off distances between the high temperature flame zone and the burning surface. Therefore, small temperature perturbations in the induction zone, which are caused by admixtures in the samples or by heat transfer between the reacting gases and the ambient medium is responsible for the different values of the stand-off distances and the high temperature flame zone and the burning surface. Among HDN, aerosols, and ADN, the most probable source of heat release in the first flame zone adjacent to the burning surface was evaluated to be dinitramidic acid. The third flame zone was caused by the decomposition of N_2O and NO and by formation of the final equilibrium products of O_2, H_2O and N_2.

ADN flame was characterized by the presence of "Dark zones" in their thermal profile [41,49–52]. ADN combustion between 5 and 20 atm exhibit two temperature plateaus, one at 600–1000 °C (1st

Please cite this article in press as: Kumar P, , An overview on properties, thermal decomposition, and combustion behavior of ADN and ADN based solid propellants, Defence Technology (2018), https://doi.org/10.1016/j.dt.2018.03.009

dark zone temperature plateau), and the other at 1000–1400 °C (2nd dark zone temperature plateau) [38]. The lower final flame temperature observed by Zenin [52] in the pressure range of 5–20 atm was possibly due to the heat losses to the surrounding medium during experiments. The temperature range of second dark zone was equal to the double base propellants and nitramine propellants [53–55].

Korobeinichev et al. [50,51], investigated on the chemical reactions of ADN in flame [50], and on the flame structure, kinetics and mechanism of the thermal decomposition by probing MS [51]. With the help of 172 chemical reactions and 31 species with its rate constants, the author modeled the ADN flame structure at 3 atm and 6 atm. They calculated the mole fractions of different species in the ADN flame zone with respect to pressure and the distance above the burning surface.

Thakre et al. [56], proposed a model of ADN monopropellant combustion with coupled condensed and gas phase kinetics and studied the physiochemical processes involved in the combustion of ADN. The model was based on the conservation equation of mass, species concentration, and energy [57,58], and takes into account finite rate chemical kinetics in both the condensed and gas-phases. Authors employed 165 reactions and 34 species in the gas phase to propose a detail chemical kinetics scheme. The burning rate was calculated and experimentally measured for the temperature range of 0.7 atm–350 atm. Previously, authors presented the combustion wave structures of RDX/GAP/BTTN in Ref. [55]. With the gas phase combustion analysis, the authors predicted the mole fractions and temperature above the burning surface at 3, 6 and 40 atm. Then they compared the results of 3 and 6 atm with Liau [59], and korobeinichev [50], which are in good agreement. The flame standoff distance was shortened sharply by increase in pressure. Pressure has little influence on ADN final combustion products, also NOx concentration in final products is less than 1%, hence making ADN a environmental propellant. They also predicted the burning rate with condensed phase combustion model too, and the measured burning rates were found to match closely with gas phase combustion model for the pressure range of 0.7–350 atm.

Ramaswamy, A.L. [49,60], studied the thermal initiation of ADN crystals and prills made by different manufacturing technique with the electron beam heating under vacuum condition [49], and did combustion experiments on prilled ADN and propellant formulations containing prilled ADN [60]. The thermal initiation of ADN crystals start with a small “reaction sites” which are about 0.01 μm in diameter. As the reaction progresses there is increase in diameter and in surface density. The “reaction sites” expands and coalesce to form a porous residue material which decomposes, leaving a hole to mark the spot or location of the electron beam heating. As the “reaction sites” expand, the shape of the sites becomes more noticeable. The sites appear to have a crystallographic nature where the shape follows that of the crystal habit on which they are formed. This “reaction sites” also termed as “nucleation” in Ref. [61]. The crystallographic shape of the “reaction sites” is indication of the fact that their formation depend on the precise position of the atoms in the crystal lattice relative to the surrounding atoms. The ADN purity, micro-structural characteristics and addition of thermal stabilizers are may be the reasons for different initiation properties.

In his 2nd paper [49], the obtained ADN propellant sample from NSWC (IH) was burned inside the ESEM and the combustion was recorded. The formulation of the propellant was not provided. It was found that the rate of regression of the polymer was far slower than that of ADN particles. In the strand burner, the burning rates are measured for 3 batches of ADN manufactured at NSWC (IH). The more spherical the prills are with higher quality or improved microstructural characteristics showed better performance. The pressure exponent (n) for irregular shaped, rhombus shaped and spherical shaped ADN are 0.38, 0.67 and 0.11–0.44 for pressure range of 35–50 atm, and 1.05, 0.58, 0.35–0.60 for pressure range of >50 atm respectively.

Hahma et al. [62], developed a melt casting technique for ADN and ADN/Al mixtures. ADN has a relatively high heat of fusion (130 kJ/kg), which makes ADN slow to melt down. The heat capacity of 1.77 kJ/(kg·K) was also very high as compared to other melt-castable explosives. The gas evolution causes ADN to froth and some foam collected on the surface, which has to be cut away after solidification of the charge. If the charge is too long, there is not enough time for the bubbles to rise to the surface, density gradients may remain in the material, and an undesirably low density is obtained at the upper part of the charge. Hence, the gas generation limits the maximum length of the charges that can be cast. ADN also shrinks by 14% of its volume upon solidification. This led to the formation of large cavity in the centre of the castings, where the material solidifies last, and to high internal tensions and a tendency to form cracks in the solid material. ADN/Al mixtures were successfully casted by adding 1% of MgO in it. The ratio of ADN/Al/MgO is 64/35/1. The theoretical mean density (TMD) for this mixture is between 95 and 99%. MgO is a good stabilizer and prevent evolution of gases from thermal decomposition of ADN. There was NH_3 gas evolution with MgO stabilized ADN. The optimal aluminum powder particle size is 10 μm for spherical and smooth particles and 50 μm for irregularly shaped powder. ADN must contain some moisture to make it melt castable and mechanically stable. Too dry ADN will crumble to pieces by itself after a few days of storage.

5. Combustion of ADN based propellants

ADN is one of the newly discovered oxidizer and it shows incompatibility issue with isocyanates (a cross linking agent used for HTPB based propellants) [63]. ADN/HTPB based propellants can be processed but their energetics is not high enough, and mechanical properties are also not good. Hence there are consistent efforts from the rocket scientific community for the selection of suitable fuel binders and plasticizers to be used with ADN for achieving maximum energy. Some of the fuel binders used with ADN are, HTPB [64–68], Polycaprolactone (PCL) [70,71], PEG-PPG [65], GAP [72–76], Desmophen [75], poly-BAMO [79], poly-NIMMO [79], PGN [79,81], Aluminum hydride [82], Paraffin [83], Hy-At [84], poly-TMPO [85], and TMPO-Tetrahydrofuran (THF) [86].

Till date numerous fuels binders are being discovered and constantly new fuels binders are being synthesized to be used with advance energetic oxidizers. The search for new fuels binders which must be compatible with available oxidizers are the areas of innovative and advance research. A summary on the types of binders in use from the early years are well documented. Some of the available non-energetic fuels binders from its early days are as follows, Black powder (1939), melted asphalt (1942), polysulfide liquid (1943), unsaturated polyesters, Poly Vinyl Chloride (PVC), polyurethanes, Polybutadiene –acrylic acid (PBAA), polybutadiene-acrylic acid acrylonitrile (PBAN, 1957), Carboxyl terminated polybutadiene (CTPB) and Hydroxyl terminated polybutadiene (HTPB) and wax. PBAN was one of the preferred fuel binders till 1975, but after the discovery of HTPB ad CTPB its usage are ruled out. AP/HTPB based propellants are still in use as we discussed earlier. With the discovery of many new high energetic oxidizers, development of new binder is also inevitable. Some of the newly synthesized energetic fuel binders are, Glycidyl azide polymer (GAP), Glycidyl nitrate (GLYN), Polyglycidyl nitrate (PGN), Polyvinyl nitrate (PVN), Polynitro phenylene (PNP), Nitratomethyl oxetane (NIMMO), Poly-NIMMO, Bis-azidomethyl oxetane (BAMO), Azidomethyl oxetane

Please cite this article in press as: Kumar P, , An overview on properties, thermal decomposition, and combustion behavior of ADN and ADN based solid propellants, Defence Technology (2018), https://doi.org/10.1016/j.dt.2018.03.009

(AMMO), Tetrahydrofuran (THF), Fluorinated polymers, Nitrated HTPB, Nitrated cyclodextrin polymers (poly-CDN), and 3-ethyl-3-(hyroxymethyl) oxetane (TMPO). Physiochemical properties of some of the binders are tabulated in Table 1.

Pang et al. [64], worked with four propellant samples with AP and ADN as oxidizers. Percentage weight of HTPB, Al, and other additives were kept constant, while the ratio of AP:ADN varied as 64:0, 54:10, 49:15, and 44:20. Experiments for measuring the burning rate of the four samples are conducted at 1, 4, 7, 10 and 15 MPa. With the increasing pressure and increasing ADN %age weight, the burning rate increases. Burning rate and pressure index for AP: ADN (44:20) at 15 MPa was 19.43 mm/s and 0.71 respectively. The other noticeable observation was the decrease in density and flame temperature with increasing ADN % age.

Chakravarthy et al. [65], prepared 13 samples of ADN/PBAN, AP/PBAN, AP/ADN/PBAN, AP/ADN/HTPB, ADN/HTPB, and AP/HTPB in different ratios, and experimentally measured the burning rate by means of combustion photography. They observed the burning surface by hot stage microscopy with the following observations:

a) The binders (PBAN and HTPB) began to melt above about 450 °C, and decomposed vigorously around 500 °C. The HTPB binder appeared to have softened prior to melting.
b) Ferric oxide was stable up to about 1000 °C.
c) In sample of cured PBAN/ADN, ADN was found to melt inside the binder. Above 140 °C, ADN began to decompose inside the solid binder; as seen by the sub-surface bubbling activity, even as the binder was turning black in those areas with predominant presence of ADN in the original sample. Gaseous decomposition products of ADN were seen to rupture through the binder and come out from binder layers suddenly at around 200 °C. The binder melts and vaporized around 480 °C, although some considerable amount of residues from the ADN sites remained.
d) With a sample of cured HTPB with ADN mixed in it, the above sequence of events was followed up to ADN decomposition, but the gases did not escape dramatically like in PBAN; instead, they caused binder to soften prematurely at lower temperature than usual. Some charred residue was left behind. Above 470 °C, the binder began to vaporize; the residue was found floating amidst the bubbling, and remained after binder vaporization.
e) When a sample of uncured (liquid) HTPB mixed with ADN was heated up to the m.p. of ADN and then cooled down. The cooling was uncontrolled, and was much lower rate than the heating. During the cooling process, the molten ADN migrate together with the uncured HTPB prepolymer, and recrystallize into a single large disk-like particle of around 1000 μm in size, back at room temperature.

Korobeinichev et al. [66,68,69], studied flame characteristics, burning rates, and final flame temperature for propellants based on ADN and HTPB at different HTPB concentrations (3–20%) in the pressure range of 0.05 MPa–0.6 MPa [60], and presented a review on the flame structure of number of energetic materials, such as AP, ADN, RDX, and HMX [68]. The summary of the investigation is presented Table 2.

For the propellants of ADN/HTPB in the ratio of 97:3 at 0.6 MPa, video images near the burning surface revealed a dark zone of 0.3 mm wide. The dark zone increased to 1.5 mm when the pressure fell to 0.1 MPa. Video records show several white, brightly luminous torches (jets) of 0.5 mm–1 mm in diameter near the burning surface. These disappeared from one site and reappeared at another. The lifetime of one of these torches was about 0.2 s. The source of luminous jet was probably the combustion of single large ADN particles formed as a result of melting and agglomeration of smaller particles. The thermocouple shows temperature fluctuations of about ±400 K at 0.1 MPa in the flame zone, within 1.5 mm–4 mm of the burning surface. Dark zone was mainly comprised of pure ADN combustion products and when this mixed with HTPB decomposition products, luminous jet flames are formed in the gas phase. The combustion products 4 mm beyond the burning surface of ADN/HTPB at 0.1 MPa are

$$0.01\ NH_3 + 0.35H_2O + 0.13\ N_2 + 0.26\ NO + 0.18\ N_2O + 0.06\ CO_2$$

The reactions in the condense phase control ADN/HTPB propellant combustion at least 0.1 MPa. However, oxidation of HTPB decomposition products in the gas phase increases the heat release there and accelerates reactions in the first and the second zones of the ADN flame.

Parr et al. [67], prepared sandwich propellants from ADN with a variety of fuels including wax, HTPB, N5, and energetic binders including GAP, and BAMO/NMMO. The diffusion flame structure of sandwich propellants studied by planar laser induced fluorescence (PLIF) and the Mie scatter imaging for sandwiches deflagrating at pressure between 1 and 14 atm. Like nitramine propellants (HMX or RDX), NO and NO_2 were initial decomposition products of ADN laminae that were consumed in the diffusion flame. The ADN sandwiches were ignited using a flux of about 150 cal/($cm^2 \cdot s$) from a CO_2 laser. At pressures below 2–3 atms, there was diffusion flame between ADN (containing N but not C), and the non-energetic fuel (containing C but not N) i.e. HTPB and candle wax. Presence of CN radicals was detected by chemiluminescence or PLIF imaging, which proved that there was a diffusion flame between the two entities. The dark zone height of ADN/HTPB and of ADN/Wax at 1 atm are 3.8 and 6.3 mm respectively. With the increasing pressure, height of dark zone decreases. Height of dark zone in ADN/HTPB sandwiches at 2 atms was 2.9 mm. At pressures above 2 or 3 atms, there was a noticeable change in the flame structure for non-energetic binders. The diffusion flame, as monitored using CN PLIF, becomes much weaker, and at 4 atm virtually disappeared. At 14 atms, the flame was nearly on the surface of the binder. With the low energy binders, wax and HTPB, nearly entire fuel lamina recovered with some charring effects. With high energetic binders too, some of the fuel was recoverable at 10 atms, despite the facts that sandwich proportions were oxidizer rich. These results indicate that in real rocket motors, ADN based CSP's will not oxidize the

Table 1
Physiochemical properties of Binders [79].

Energetic binders	ΔH_f/(kJ·mole^{-1})	OB/%	ρ/(g·cm^{-3})	Glass transition temp/°C
GAP	+117	−121	1.3	−50
Poly-BAMO	+413	−124	1.3	−39
Poly-AMMO	+18	−170	1.06	−35
Poly-NIMMO	−335	−114	1.26	−25
PGN	−285	−61	1.39	−35
HTPB	−62	−324	0.92	−65

Please cite this article in press as: Kumar P, , An overview on properties, thermal decomposition, and combustion behavior of ADN and ADN based solid propellants, Defence Technology (2018), https://doi.org/10.1016/j.dt.2018.03.009

Table 2
Visual flame characteristics, burn rates, and final flame temperature of ADN/HTPB propellants [66].

Composition of propellant AND/HTPB	Pressure/ MPa	Burning rate/ ($mm \cdot s^{-1}$)	Final temp./K	Visual characteristics
80/20	0.1	~0.9	*	Carbonaceous bubbles at burning surface
90/10	0.1	~1.5	*	Carbonaceous carcass in some places at burning surface of the strand
90/10	0.3	~3.4	*	
93/7	0.6	~7.3	>3300	Height of luminous zone ~5 cm
97/3	0.6	~7.5	*	Dark zone of ~0.3 mm
97/3	0.1	~1.2	≈2400	Luminous flame jets with characteristic dimensions less than 1 mm diameter and characteristic lifetime of ~0.2s.

fuel in a diffusion flame close to the surface. Therefore there was no particle size effect on burning rate or we can say there is a negative particle size effect as the binder acts as a heat sink for the smaller diameter ADN particles.

Korobeinichev et al. [70], investigated characteristics and mechanics of combustion for ADN/PCL (polycapro-lactone) propellants. ADN of 40 μm size and two types of PCL with molecular weights of 10,000 (flake form, m.p. 333 K), and 1250 (waxy solid, m.p. 309–321 K) are used in 4 propellant formulations. The formulations are, a) ADN-PCL (10000), b) ADN-PCL (1250), c) ADN-PCL (10000) + 2% CuO, and d) ADN-PCL (1250) + 2% CuO. Video recordings of the combustion of ADN-PCL (1250) propellants shows the presence of dark zone near the combustion surface. The thickness of the dark zone varies from 1 mm near the origin of the flamelet to 3–4 mm in the space between flamelets. Three zones exist in the flame at 0.1 MPa, a) a narrow dark zone (0.2 mm–0.3 mm, 600 K–1150 K), b) a dark zone (0.5 mm- 3 mm, 1150 K– 1450 K), c) luminous zone (4–8 mm, 2600 K).

Jones et al. [73], performed characterization of ADN crystals, ADN prills and two ADN/GAP propellants with ion chromatography (IC) to check purity of ADN crystals and prills, DSC to study thermal behavior, TG-DTA-FTIR-MS for gas detection when sample decompose, accelerating rate calorimeter (ARC), heat flux calorimeter (HFC), and isothermal nanocalorimetry (INC) to study the stability, electrostatic discharge (ESD), and Impact machine to study the sensitivity. The DSC, TGA, FTIR, and MS results of ADN crystals and prills are similar to the reported ones in other literature. FTIR results of two propellants showed the presence of N_2O, NO_2, CO_2, HCN, and CO_2. Calculated activation energy from ARC for the ADN crystals, ADN prills, prop A and prop B are 257 ± 9, 310 ± 9, 324 ± 14 and 405 ± 78 kJ/mol.

Kuibida et al. [74], studied flame structure of CSP's and sandwiches based on ADN/GAP at pressure range of 0.015 MPa–0.3 MPa with molecular beam mass spectrometry. Sandwiches propellants are not used in real rocket motors but are more convenient for studying the flame structure and for computer simulations. Two types of sandwiches with various lamina thickness was prepared for the present study. 1st sandwich consisted of five 0.8 mm thick ADN laminae and six 0.2 mm thick laminae of cured GAP, and 2nd sandwich consisted of three 1.6 mm ADN laminae, two 0.4 mm GAP laminae between them and two another 0.2 mm GAP laminae at the ends. Two zones in a flame were found, a) near to the burning surface is dark, low temperature zone of width of 1.5 mm. This zone is similar to the first zone in a flame of pure ADN at pressure of 3 atms, in which dissociation of ADN vapors to ammonia and dinitramidic acid takes place, b) luminous zone with a width of 8–10 mm, where further oxidation of decomposition products of the sandwich's combustion takes place.

Landsem et al. [71], tried to improve the mechanical properties of ADN based CSP's by incorporation of HMX and a neutral polymeric bonding agent, NPBA. They prepared total of 3 propellant samples with following formulations, a) ADN-HMX-GAP-TMETN + NPBA, b) ADN-HMX-GAP-HTCE-TMETN + NPBA, and c) ADN-HMX-HTCE-TMETN + NPBA, and then did tensile testing on them. Unmodified CSP's based on ADN, GAP binder, and energetic nitrate ester plasticizers have poor mechanical tensile strength of barely 0.20 MPa. The prepared propellant samples show good mechanical properties and the observed mechanical properties of the three propellant samples are shown in Table 3.

Cerri et al. [75], performed stress and strain analysis, dewetting phenomena, compatibility issues with various plasticizers and curing agents, and evaluation of glass temperature of ADN/GAP, and ADN/Desmophen propellants. Total of 12 propellant formulations were made, 4 of ADN-GAP, AP-GAP and ADN-Desmophen each. GAP based propellants do not have satisfactory mechanical properties as compared to formulations containing Desmophen. Usage of N100 as curing agent for GAP-diol pre-polymers showed improved mechanical properties. SEM analysis of the ADN/GAP based formulations showed evidence of a high porosity of the propellants and strong dewetting phenomena. ADN based propellants showed remarkable chemical decomposition. Mass loss measurements revealed an acceleratory behavior at high temperature values.

Menke et al. [77], prepared 3 ADN-GAP propellants and 2 AP-GAP propellants with addition of HMX in all the propellants with varying % age. They used TMETN as a plasticizer in some propellants. They prepared ADN-GAP propellants with isocyanate curing to reveal the reasons for ADN incompatibility with isocyanates. During the curing reaction between ADN and isocyanates at 60 C, the major gaseous product CO_2 originate from the NCO reaction with proton acid or water as both. Hydrolytic splitting of ADN to NH_3 and DA plays a key role in reaction with isocyanates. The resulting ADN-GAP propellant with isocyantes is very soft foams after mixing and curing at 60 °C. It in concluded that stabilizers for isocyanate curing of ADN propellants should:

a) Bind acids like DA and possibly HNO_3, originating from ADN decomposition.
b) Bind or remove water and NH_3 from the curing reaction.

ADN/HMX/GAP based minimum smoke propellants with Isp >2500 was successfully formulated, either cured by tri-isocyanate N100 or with BPS. Incompatibility of ADN with isocyanates can be overcome by a mixture of stabilizers consisting of a NE stabilizer, a water and an ammonia adsorbing agent, and a base like MNA

Table 3
Mechanical properties of prepared propellant samples [71].

Mechanical properties (21 C)	Prop A	Prop B	Prop C
Max tensile strength/MPa	0.42	0.48	0.50
Strength at break/MPa	0.40	0.44	0.49
Elongation at σ_{max}/%	26.5	23.0	35.0
Elongation at break/%	28.3	23.6	35.2
Elastic modulus/MPa	5.6	9.0	8.4
Shore A hardness	69	92	80

Please cite this article in press as: Kumar P, , An overview on properties, thermal decomposition, and combustion behavior of ADN and ADN based solid propellants, Defence Technology (2018), https://doi.org/10.1016/j.dt.2018.03.009

which was able to neutralize DA at the surface of ADN prills without being decomposed by its oxidizing power. Overall, three ADN-HMX-GAP propellants with 15–20% HMX of energetic solids, one with isocyanate N100 curing and TMETN plasticizer, and two with BPS curing with and without TMETN plasticizer have been casted and cured successfully. Due to lower molecular weight of the exhaust gases, the ADN-GAP formulations deliver highest Isp than the AP-GAP propellants. The burn rates of the investigated ADN-GAP propellants lie between 25 and 32 mm/s at 100 atms, which is nearly 20% higher than AP-GAP propellants. But in the study, AP particles sizes were 45 and 200 μm, and hence AP-GAP burning rate can be increased by using AP of finer sizes. Chemical stability of ADN-GAP is also better then AP-GAP as measured by Dutch test and vacuum stability. The major advantage associated with ADN-GAP propellants is its high thermodynamic (as suggested by DSC) and good burning performance. Disadvantages associated are, high thermal sensitivity, and early tendency to deflagration and possibly to detonation.

Currently Hydrazine is the major monopropellant used in liquid rocket propulsion. Larsson [78], prepared a liquid monopropellant sample based on ADN [FLP-106] to replace hydrazine. The composition of FLP-106 is low volatile fuel, water and 64.6% ADN. It is a low-viscous yellowish liquid, with high performance, low vapor pressure and low sensitivity. Low volatile fuels included, 1,4-butanediol, glycerol, ethylene glycol, and trimethyl propane. The comparison of the properties of hydrazine and FLP-106 is tabulated in Table 4.

To replace hydrazine by FLP-106, it is necessary that it must be ignite easily. When FLP-106 drop put on a hot place (200–250 °C), it ignites and burns fast. This shows that the thermal ignition is possible. In Ref. [78], authors performed experiments with electrical energy ignition of FLP-105 and FLP-106. These samples were heated by a current forced through it i.e. by resistive heating. Light signals from the optical fibers indicate that the propellant is ignited. From high speed video recordings it was observed that the ignition first starts at the lower electrode (cathode), followed by ignition at the upper electrode (anode). The required energy was lower than the expected, thus ADN-based monopropellant has the potential to replace hydrazine.

ADN combined with GAP/poly-BAMO/poly-BAMO/poly-NIMMO/PGN can offer specific impulse upto 300s or more. While AP-BAMO/NIMMO propellant has a specific impulse of 265 s. Talawar [80] in his review paper, summarized specific impulse of ADN with various high energetic binders in his review paper. The specific impulse of ADN-GAP, ADN-poly-BAMO, ADN-poly-NIMMO, ADN-PGN, ADN-GAP-Al are 310, 312, 309, 306, and 274.2 respectively.

Effects of aluminum halide (AlH_3) and of Al on the specific impulse of the mixtures are presented in Ref. [82]. 20% AlH_3 in 85%, 87% and 89% solids loading of ADN gives the specific impulse of 282, 285 and 288 s respectively. Similarly 20% Al on same loading of solids ADN gives the specific impulse of 273s in all the cases, while in 90% AP loading the specific impulse was 264s.

Table 4
Properties of hydrazine and FLP-106 at 25 °C [78].

Property parameter	Hydrazine	FLP-106
Specific impulse/s	230	259
Density/(g·cm^{-3})	1.0037	1.357
Temp. in chamber/°C	1120	1880
Viscosity/(cP)	0.913	3.7
Thermal expansion co-efficient/K^{-1}	9.538×10^{-4}	6.04×10^{-4}
Heat capacity/(J·g^{-1}K^{-1})	3.0778	2.41
Mass density	–	$1.378-8.2 \times 10^{-4}$T

Weiser et al. [83], investigated on the burning rate, UV/Vis spectrum at a pressure of 0.5 MPa, temperature in the reaction zone at 0.5 MPa, IR emission spectra in the flame zone and species profile over the burning surface of ADN/Paraffin mixtures. The burning rate of pure ADN was higher than ADN/Paraffin mixtures from 0.5 MPa to 5 MPa, and afterwards burning rate of ADN/Paraffin was higher. The burning rates of ADN/Paraffin at 0.5 MPa and at 10 MPa were 7 mm/s and 80 mm/s. UV/Vis spectrum shows the presence of OH, CN, and NH in the decomposition products of ADN/Paraffin at a pressure of 0.5 MPa. Species profiles over the burning surface of ADN/Paraffin shows the presence of H_2O, CO, CO_2, and NO. CO increases more rapidly than H_2O and CO, which rises approximately linear above the surface. The concentration of CO reaches the maximum at 7 mm above the surface and those of CO_2, and H_2O at 5 mm–10 mm. NO reaches the maximum intensity at 3 mm and then vanishes at the height of 7 mm. NO was the main oxidizing agent in the flame of ADN/paraffin. Maximum flame temperature observed was nearly 2960 K.

Lembert and Manelis in his two part papers [87,88], discussed on the various formulations for the development of environmentally safe solid composite propellants [88], and theoretical predicted the energy potentials of AN, AP, and ADN with four different binders namely, hydrocarbon binder (HB) [$\Delta H_f = -390$ kJ/kg, $\rho = 0.91$ g/cm^3, Hydrogen content = 12%], poly (methylvinyltetrazolate) (PMVT) [[$\Delta H_f = +1255$ kJ/kg, $\rho = 1.28$ g/cm^3, Nitrogen content = 46%], active binder (AB) [[$\Delta H_f = -757$ kJ/kg, $\rho = 1.49$ g/cm^3, Oxygen content = 47%] and poly (vinylmethoxydiazen-N-oxide) (PVMDO) [[$\Delta H_f = 0$ kJ/kg, $\rho = 1.31$ g/cm^3, Hydrogen content = 6% and oxygen content = 31%] [87].

In Ref. [87], authors prepared propellant formulations with AN, AP, and ADN with same four binders and theoretically calculated the energy potentials. Further, they added 20% Al and 13% Be in the formulation and calculated the energy potential again. In the same paper, AN stabilization were also carried out with uric acid, isatine, guanine, and nitrouracile. In Ref. [88], authors presented the formulations of these 4 binders with 3 dinitramide salts, HMX, octanitrocubane, nitroform salts, organic oxidizers and methylenedinitramine. Further they added 25% Aluminum hydride in the ADN formulations and again theoretically calculated the energy parameters.

In the recent years, experimental studies and feasibility of ADN as a suitable oxidizer for monopropellant thruster is getting much attention [93–99]. As discussed previously, the main aim to utilize ADN in liquid rocket motor is to replace hydrazine and hydrazine based compounds which are carcinogenic in nature and also required costly materials to store them. Small scale thruster is generally used to study the amount of thrust generation, gaseous composition, pressure inside motor, flame temperature, decomposition and combustion mechanism etc [93,94]. Catalyst and catalytic bed were also used to improve the combustion properties and to enhance the ballistic properties of ADN based monopropellant thrusters [95,96]. It was observed that, nitrous oxide (N_2O) play important role in controlling the burning rate of ADN based liquid fuels [97]. RHEFORM is one global initiative which is working to enable the replacement of hydrazine with liquid propellants based on ammonium dinitramide (ADN) [998]. In Ref. [99], numerical simulation of ammonium dinitramide (ADN)-based non-toxic aerospace propellant decomposition and combustion in a monopropellant thruster. The obtained results are very positive and in future ADN has the potential to replace hydrazine in all kind of liquid rocket engines. Combustion studies of gelled ADN is also a new approach to use it more efficiently by increasing the density of liquid ADN [100].

Combustion and decomposition mechanism of ADN is mostly controlled by condensed phase combustion [101] as stated by

Please cite this article in press as: Kumar P, , An overview on properties, thermal decomposition, and combustion behavior of ADN and ADN based solid propellants, Defence Technology (2018), https://doi.org/10.1016/j.dt.2018.03.009

several authors, as we discussed previously. Above discussion provide some insight into the vast area of propellant technology. To develop high performance propellants based on new oxidizers like ADN in the present case, it required undeterred efforts and years of expertise. In the coming future, the scope of green propellants in rocketry should be in their full phase, and hence, technology for the pilot scale production of ADN based propellants should be ready.

6. Compilation of ADN properties

Important physical and chemical properties of ADN are summarized in Table 5.

7. Conclusion

ADN is a compound of interest for rocket community along with in energetic materials community too. Also, since ADN can be utilized in both solid and liquid propelled rockets, which further provides an impetus to continue research programs over it. Further, dinitramide anion and various other compounds based on it also play an important role in various types of applications [102]. Due to such reasons, a thorough knowledge on ADN from various chemical and physical aspects is an important step. Some of the important points on the decomposition and combustion properties of ADN from previous literature are summarized below:

a) Thermal decomposition of ADN depends on pressure, temperature, storage time, and on the experimental techniques. Decomposition of ADN is generally acid-catalytic and self-accelerated. There is formation of huge amounts of AN and N_2O due to solid-phase dissociation.
b) Temperature measurements show a 3-phase zone structure of the ADN flame. The ADN surface temperature is the temperature of dissociation of AN. ADN combustion is characterized by intense energy release in condensed phase, weak heat feedback from the gas phase, and high burning rate.
c) Major decomposition of ADN completed by 200 °C.
d) AN forms a eutectic mixture with ADN during storage, and because of this eutectic mixture, the m.p. of ADN drops below from 93 °C.
e) ADN decomposes into NH_3 (Ammonia) and $HN(NO_2)_2$ (dinitramidic acid) in its first stage.
f) In strong acids, such as H_2SO_4, and HNO_3, ADN decomposes more rapidly at room temperature as the rate of acid-

Table 5
Compilation of ADN properties.

Parameter	Value(s)	Reference(s)
Formula	$NH_4N(NO_2)_2$	[7]
Molecular weight	124.07	[12]
Morphology of crystal	needles	[11]
Color	transparent	[89]
Heat of formation	−148 kJ/mol, −35.4 kcal/mol	[12,72] [25]
Heat of combustion	101.3 kcal/mol	[25]
Heat of vaporization	155.4 ± 12.6 kJ/mol	[27]
Heat capacity	1.8 J/g	[25,62]
Eectrostatic discharge sensitivity	0.45 J	[25]
Heat of melting	142 J/g	[72]
Heat of solution	35.7 kJ/mol	[72]
Heat of fusion	130 ± 5 J/kg	[62]
Molar volume (liquid)	74.08 g/mol	[72]
Oxygen balance	26%	[80]
Hygroscopicity	High	[11]
Critical relative humidity	55.2%	[72]
Density (solid)	1.81 g/cm^3	[72]
Density (liquid)	1.675 g/cm^3	[72]
Melting point	92-95 °C	[11]
Decomposition point	150 C (onset) to 230 C (end of exotherm)	[62]
Coefficient of thermal expansion	1.91×10^{-4} K^{-1}	[62]
Shrinkage on solidification	14%	[62]
Sensitivity, a)Drop weight (RDX)	31 cm (38 cm), powder	[7]
b)Friction test (RDX)	59 cm (38 cm), prilled >35 kp (12 kp)	
Major raman peaks (relative intensities)	495 cm^{-1} (0.063), 833 cm^{-1} (0.183) 958 cm^{-1} (0.051), 1178 cm^{-1}(0.047) 1338 cm^{-1} (0.230)	[7]
UV peaks	214 nm, 284 nm	[7]
Molar absorption co-efficients	$\mathcal{E}_{214} = 6680$ Lmole^{-1}cm^{-1} $\mathcal{E}_{284} = 5500$ Lmole^{-1}cm^{-1}	[7]
Solubility in water (20 °C)/wt%	78.1	[10]
Classification	1.1 explosive	[89]
System	Monoclinic	[12]
Space group	$P2_1/c$	[12]
a, b, c (Å)	6.914, 11.787, 5.614	[12]
α, β, ϒ (deg)	90, 100.4, 90	[12,90]
V (Å^3)	450	[12]
Z	4	[12]
Crystal shape	prism	[12]
Absorption co-efficient	0.1798 mm^{-1}	[91]
Toxicity	Mild	[25]
Thermal conductivity of solid	.001 cal/cm/s/K	[92]
Thermal conductivity (condensed phase)	0.00193 cal/cm/s/K	[92]
Thermal diffusivity	1.78×10^{-7} m^2/s	[92]

Please cite this article in press as: Kumar P, , An overview on properties, thermal decomposition, and combustion behavior of ADN and ADN based solid propellants, Defence Technology (2018), https://doi.org/10.1016/j.dt.2018.03.009

catalytic decomposition is proportional to acidity. The NO_2 gas was found to catalyze ADN decomposition, whereas the basic substances, such as NH_3, NH_4F, amine, and urea may restrain ADN decomposition.

g) NH_3, $HN(NO_2)_2$, $HNNO_2$, HNO_3, N_2O, NO_2, NO, H_2O, N_2 and AN are found to be the prominent decomposition products of ADN pyrolysis, and their evolution rates depend on temperature and pressure.

h) N_2O evolution is one of the main characteristics of ADN thermal decomposition.

i) Activation energy for ADN was 175 ± 20 kJ/mol, which decreases to 125 ± 20 kJ/mol at the completion of the reaction.

j) ADN has high heat of decomposition, which led to high burning rate.

k) The dissociation temperature of ammonium nitrite is lower than that of the other ammonium salts, ADN and AN.

l) ADN combustion mostly governs by condensed phase mechanism.

m) Flameless combustion is characteristics of energetic material at low pressures. As the pressure increases a high temperature flame appears. Combustion is controlled by c-phase reactions if the heat flux from the gas phase can be neglected i.e. if the heat flux from the gas phase is much smaller than the heat flux into the depth of the condensed phase. The most important parameters of the c-phase model are the surface temperature and the kinetics of the c-phase reaction controlling the burning rate.

n) ADN flame is characterized by the presence of “Dark zones” in its profile

o) Torch like flames (or flamelets) are the characteristic of ADN and ADN based CSP's combustion.

p) ADN can also replace hydrazine in coming future. ADN already has the potential to replace AP in coming future.

References

[1] Larsson A, Wingborg N. Green propellants based on ammonium dinitramide (ADN). In: Jason Hall Dr, editor. Advances in spacecraft technologies; 2011. ISBN: 978-953-307-551-8.
[2] Venkatachalam S, Santhosh G, Ninan K. Propellants Explos Pyrotech 2004;29(3):178–87.
[3] Jacobs PWM, Whitehead HM. Chem Rev 1969;69(4):551–90.
[4] Santhosh G, Venkatachalam S, Kanakavel M, Ninan KN. Indian J Chem Tech 2002;9:223–6.
[5] Klapotke TM, Mayer P, Schulz A, Weigand JJ. J Am Chem Soc 2005;12:2032–3.
[6] Bottaro JC, Penwell PE, Schmitt RJ. J Am Chem Soc 1997;119:9405–10.
[7] Ostmark H, Bemm U, Langlet A, Sanden R, Wingborg NJ. Energetic mater. 2000;18:123–38.
[8] Andreev AB, Anikin OV, Ivanov AP, Krylov VK, Pak ZP. Russ Chem Bull (International edition) 2000;49(12):1974–6.
[9] Mishra IB, Russll TB. ThermochimD Acta 2002;384:47–56.
[10] Matsunga H, Habu H, Miyake AJ. Therm. Anal. Calorim 2013;111:1183–8.
[11] Nagamachi MY, Oliveira JIS, Kawamoto AM, Dutra RCL. J Aero Technol Manag 2009;1(2):153–60.
[12] Gilardi R, Anderson JF, George C, Butcher RJ. J Am Chem Soc 1997;119:9411–6.
[13] Oxley JC, Smith JL, Zheng W, Rogers E, Coburn MD. J Phys Chem A 1997;101:5646–52.
[14] Pavlov AN, Nazin G. Russ Chem Bull 1997;47(11):1848–50.
[15] Politzer P, Seminario JM, Concha MC. J Mol Struct (Thermochem) 1998;427:123–9.
[16] Vyazovkin S, Wight CA. J Phys Chem A 1997;101:5653–8.
[17] Lobbecke S, Krause HH, Pfeil A. Propellants, Explos Pyrotech 1997;22:184–8.
[18] Kumar P, Joshi PC, Kumar R. Combust Flame 2016;166:316–32.
[19] Yang R, Thakre P, Yang V. Combust. Explo. Shock+ 2005;41(6):657–79.
[20] Andreev AB, Anikin OV, Ivanov AP, Krylov VK, Pak ZP. Russ Chem Bull (International edition) 2000;49(12):1974–6.
[21] Rossi MJ, McMillen DF, Golden DM. SRI project 8999, Office of naval research. 1992.
[22] Ermolin NE. Combust. Explo. Shock+ 2004;40(1):92–109.
[23] Park J, Chakraborty D, Lin MC. Twenty-Seventh symposium (International) on combustion. The combustion institute; 1998. p. 2351–7.
[24] Rahm M, Brinck TJ. Phys Chem A 2010;114:2845–54.
[25] Rahm M. Doctoral thesis. Stockholm: KTH Chemical sciences and engineering; 2010.
[26] Pavlov AN, Grebennikov VN, Nazina LD, Nazin GM, Manelis GB. Russ Chem Bull 1999;48(1):50–4.
[27] Shmakov AG, Korobeinichev OP, Bol'shova TA. Combust. Explo. Shock+ 2002;38(3):284–94.
[28] Brill TB, Brush PJ, Patil DG. Combust Flame 1993;92:178–86.
[29] Vyazovkin S, Wight CA. J Phys Chem A 1997;101:7217–21.
[30] Zhu RS, Chen HL, Lin MC. J Phys Chem A 2012;116:10836–41.
[31] Lobbecke S, Krause HH, Pfeil A. Propellants, Explos Pyrotech 1997;22:184–8.
[32] Matsunaga H, Habu H, Miyake AJ. Therm. Anal. Calorim 2014;116:1227–32.
[33] Matsunaga H, Izato Y, Habu H, Miyake AJ. Therm. Anal. Calorim 2015;121:319–26.
[34] Izato Y, Koshi M, Miyake A, Habu HJ. Therm. Anal. Calorim 2017;127:255–64.
[35] Muravyev NV, Koga N, Meerov DB, Pivkina AA. Phys Chem Chem Phys 2017;19:3254–64.
[36] Kleimark J, Delanoe R, Demaire A, Brinck T. Theor. Chem. Acc 2013;132:1412–20.
[37] Ermolin NE, Fomin VM. Combust Explos Shock Waves 2016;52(5):566–86.
[38] Sinditskii VP, Egorshev VY, Levshenko AI, Serushkin VV. J Propul Power 2006;22(4):769–76.
[39] Sinditskii VP, Egorshev VY, Levshenko AI, Serushkin VV. J Propul Power 2006;22(4):777–84.
[40] Sinditskii VP, Egorshev VY, Serushkin VV, Filatov SA. Combust. Explo. Shock+ 2012;48(1):81–99.
[41] Fetherolf BL, Litzinger TA. Combust Flame 1998;114:515–30.
[42] Sinditskii VP, Egorshev VY, Serushkin VV, Levshenkov AI. 8th International workshop on combustion and propulsion, Naples, Italy. 2002.
[43] Sinditskii VP, Fogelzang AE, Levshenkov AI, Egorshev VY, Serushkin VV. AIAA 36th aerospace sciences meeting and exhibit, Reno, NV, AIAA-98–0808. 1998.
[44] Parr TP, Hanson-Parr DM. In: 23rd JANNAF combustion meetingvol. 1; 1986. p. 249–67 (457).
[45] Merzhanov AG. Combust Flame 1969;13(2):143–56.
[46] Fujisato K, Hiroto H, Miyake A, Hori K, Vorozhtsov AB. Propellants, Explos Pyrotech 2010;35:1–8.
[47] Strunin VA, Diyakov AP, Manelis GB. Combust Flame 1999;117:429–34.
[48] Ermolin NE. Combust. Explo. Shock+ 2007;43(5):549–61.
[49] Ramaswamy AL. Combust. Explo. Shock+ 2000;36(1):119–24.
[50] Korobeinichev OP, Bolshova TA, Paletsky AA. Combust Flame 2001;126:1516–23.
[51] Korobeinichev OP, Kuibida LV, Paletsky AA, Shmakov AG. Int J Energetic Mater Chem Propuls 1997;4(1–6):38–47.
[52] Zenin AA, Puchkov VM, Finjakov SV. AIAA paper No. 99–0595. 1999.
[53] Yang R, Thakre P, Liau Y, Yang V. Combust Flame 2006;145:38–58.
[54] Anderson WR, Meagher NE, Vanderhoff JA. Combust Flame 2011;158:1228–44.
[55] Yoon JK, Thakre P, Yang V. Combust Flame 2006;145:300–15.
[56] Thakre P, Yi Duan, Yang V. Combust Flame 2014;161:347–62.
[57] Bilger RW, Jia X, Ll JD, Nguyen TT. Combust Sci Technol 1996;115(1):1–39.
[58] Prasad K, Yetter RA, Smooke MD. Combust Sci Technol 1997;124(1–6):35–82.
[59] Liau YC, Yang V, Lin MC, Park J. In: 35th JANNAF combustion meeting; 1998. p. 13–30. CPIA Publication No. 685(2).
[60] Ramaswamy AL. J Energetic Mater 2000;18(1):39–60.
[61] Teipel U. Heintz T. Propell. Explos. Pyrot 2005;30(6):404–11.
[62] Hahma A, Edvinsson H, Ostmark HJ. Energ. Mater 2010;28:114–38.
[63] Landsem E, Jensen TL, Hansen FK, Unneberg E, Kristensen TE. Propellants, Explos Pyrotech 2012;37:691–8.
[64] Pang W, Fan X, Zhang W, Xu H, Wu S, Liu F, Xie W, Yan NJ. Chem Sci Technol 2013;2(2):53–60.
[65] Chakravarthy SR, Freeman JM, Price EW, Sigman RK. Propellants, Explos Pyrotech 2004;29(4):220–30.
[66] Korobeinichev OP, Paletsky AP. Combust Flame 2001;127:2059–65.
[67] Parr T, Parr DH. In: 30th JANNAF combustion subcommittee meeting, vol. II; 1993.
[68] Korobeinichev OP, Paletskii AA, Volkov EN. Russ J Phys Chem B 2008;2(2):206–28.
[69] Korobeinichev OP, Kuibida LV, Paletsky AA, Shmakov AA. J Propul Power 1998;14:991–1000.
[70] Korobeinichev OP, Paletskii AA, Tereschenko AG, Volkov EN. Proc Combust Inst 2002;29:2955–61.
[71] Landsem E, Jensen TL, Hansen FK, Unneberg E, Kristensen TE. Propellants, Explos Pyrotech 2012;37:691–8.
[72] Larrson A, Niklas W. Advances in spacecraft technologies, FOI, Swedish defence research academy, Sweden.
[73] Jones DEG, Kwok QSM, Vachom M, Badeen C, Ridley W. Propellants, Explos Pyrotech 2005;30(2):140–7.
[74] Kuibida LV, Korobeinichev OP, Shmakov AG, Paletskii AA, Volkov EN. Combust Flame 2001;126:1655–61.
[75] Cerri S, Bohn MA, Menke K, Galfeti L. Propellants, Explos Pyrotech 2013;38(2):190–8.
[76] Wingborg N, Andreasson S, Flon J, Johnsson M, Liljedahl M. 46th AIAA/ASME/SAE/ASEE joint propulsion conference and exhibit. 2010. p. 1–8.
[77] Menke K, Heintz T, Schweikert W, Keicher T, Krause H. Propellants, Explos

Please cite this article in press as: Kumar P, , An overview on properties, thermal decomposition, and combustion behavior of ADN and ADN based solid propellants, Defence Technology (2018), https://doi.org/10.1016/j.dt.2018.03.009

Pyrotech 2009;34:218–30.
[78] Larsson A, Wingborg N, Elfsberg M, Appelgren P. FOI-Swedish defence research agency, Sweden.
[79] Talawar MB, Sivabalan R, Anniyappan M, Gore GM, Asthana SN, Gandhe BR. Combust Explo Shock+ 2007;43(1):62–72.
[80] Talawar MB, Sivabalan R, Mukundan T, Muthurajan H, Sikder AK, Gandhe BR, Rao A. J Hazard Mater 2009;161:589–607.
[81] Hinshaw, et al. United state patent 1996; Patent No. 5498303.
[82] Agrawal JP. In: High energy materials: propellants, explosives and pyrotechnics. Wiley Publications; 2010.
[83] Weiser V, Eisenreich N, Baier A, Eckl W. Propellants, Explos Pyrotech 1999;24:163–7.
[84] Nair UR, Asthana SN, Subhananda R, Gandhe BR. Defence Sci J 2010;60(2):137–51.
[85] Rahm M, Westlund R, Eldster C, Malmstrom EJ. Pol Sci Part A, Poly Chem 2009;47(22):6191–200.
[86] Rahm M, Malmstrom E, Eldsater CJ. App Poly Sc 2011;122:1–11.
[87] Manelis GB, Lempert DB. Prog Propul Phys. 2009;1:81–96.
[88] Lempert DB, Manelis GB, Nechiporenko GN. Prog Propul Phys. 2009;1:63–80.
[89] Ing Dr, editor. Crystallization of the energetic oxidizer salt ammonium dinitramide: theoretical and experimental considerations. Germany: Fraunhofer institute for chemical technology; 2008. PHD Thesis.
[90] Valerdez GF, Alavi S, Thompson DL. J Chem Phys 2003;119(13):6698–708.
[91] Ritchie JP, Zhurova EA, Matin A, Pinkerton AA. J Phys Chem 2003;107:14576–89.
[92] Gross ML, editor. Two dimensional modeling of AP/HTPB utilizing a vorticity formulation and one- dimensional modeling of AP and AND. Brigham young university; 2007. PHD Thesis.
[93] Jing L, You X, Huo J, Zhu M, Yao Z. Aero Sci Technol 2017;69:161–70.
[94] Chen J, Li G, Zhang T, Wang M, Yu Y. Acta Astronaut 2016;129:367–73.
[95] Yu Y, Li G, Zhang T, Chen J, Wang M. Energy Convers Manag 2015;106:566–75.
[96] Zhang T, Li G, Yu Y, Chen J, Wang M. Combust Sci Technol 2016;188(6):910–23.
[97] Zeng H, Li F, Zhang S, Yu XJ. Propul Power 2016;31(5):1496–500.
[98] Negri M, Wilhelm M, Hendrich C, Wingborg N, Gediminas L, Adelow L, Maleix C, Chabernaud P, Brahmi R, Beauchet R, Batonneau Y, Kappenstein C, Koopmas R, Schuh S, Bartok T, Scharlemann C, Gotzig U, Schwentenwein M. Acta Actronaut 2018;143:105–17.
[99] Zhang T, Li G, Yu Y, Sun Z, Wang M, Chen J. Energy Convers Manag 2014;87:965–74.
[100] Guan H, Li G, Zhang N. Acta Astronaut 2018;144:119–25.
[101] Fujisato K, Habu H, Hori K. Propellants, Explos Pyrotech 2014;39:714–22.
[102] Vandel AP, Lobanova AA, Loginova VS. Application of dinitramide salts (review). Russ J Appl Chem 2009;82(10):1763–8.

Please cite this article in press as: Kumar P, , An overview on properties, thermal decomposition, and combustion behavior of ADN and ADN based solid propellants, Defence Technology (2018), https://doi.org/10.1016/j.dt.2018.03.009